Japanese Journal of Applied Physics
Vol. 46, No. 10A, 2007, pp. 6634–6638

Electrically Tunable Three-Dimensional Holographic Photonic Crystal Made of Polymer-Dispersed Liquid Crystals Using a Single Prism

Yan Jun LIU and Xiao Wei SUN*

School of Electrical and Electronic Engineering, Nanyang Technological University, Nanyang Avenue, Singapore 639798, Singapore

(Received May 16, 2007; accepted July 25, 2007; published online October 9, 2007)

An electrically tunable three-dimensional holographic photonic crystal made of polymer-dispersed liquid crystals was fabricated using a specially designed prism. This prism split a collimated laser beam into four beams which interfered with each other at the base of the prism to form a three-dimensional spatial light intensity pattern. The spatial light intensity pattern was then recorded inside a cell filled with polymer-dispersed liquid crystals to create photonic crystal structures, which were examined by atomic force microscopy and scanning electron microscopy. The diffraction and electrically tunable properties were also presented. The electro-optical response time was also measured. [DOI: 10.1143/JJAP.46.6634]

KEYWORDS: photonic crystal, polymer-dispersed liquid crystal, holographic interference, electro-optical response

1. Introduction

The existence of photonic bandgap (PBG), a region in frequency domain where propagating modes are forbidden, in photonic crystals (PhCs)[1,2] makes it potentially useful in visible and near infrared (NIR) regions, such as enhancing the brightness of light-emitting diodes (LEDs),[3] fabricating highly integrated waveguides,[4] and filters,[5] etc. Different approaches have been used to fabricate PhCs, such as electron-beam lithography,[6] self-organization of colloids,[7] layer-by-layer micromachining,[8] and holographic lithography.[9–15] Among these methods, laser holography technique offers a highly versatile and flexible approach to create organic PBGs; laser holography is able to create large area periodic structures through an exposure process, while maintaining the uniformity of the period, and offering more degrees of freedom to control the structures. It has been demonstrated both theoretically and experimentally that three-dimensional (3D) structures can be obtained by recording the interference patterns generated by multiple coherent laser beams on photosensitive materials.[12,16] Generally, a high refractive index contrast is required for a full PBG. However, materials with relatively low index contrasts, especially for organic materials, can also find applications that make use of their refraction properties, e.g., superprism effect.[17]

On the other hand, it is advantageous if the PBGs of PhCs can be tuned. Inoue *et al.* showed that the optical nonlinearities could be tuned by changing the dispersion and the group velocity of PBGs.[18] As is known, liquid crystal (LC)-based PhC is inherently tunable under external stimuli, such as electric field and heat. Holographic polymer-dispersed liquid crystal (H-PDLC) material[19] is a new kind of material, which can be photo-polymerized by UV or visible lasers, depending on the chosen materials. It has attracted great attention due to a wide range of potential applications, such as reflective flat-panel displays,[20–22] switchable lenses,[23] optical switches,[24,25] organic lasers,[26–28] etc. Recently, much interest was focused on fabricating PhCs based on H-PDLC. Many two-dimensional (2D) and 3D PhCs have been demonstrated using H-PDLC materials, including transverse square,[29,30] orthorhombic,[31,32] and diamond-like lattices.[33] However, to achieve these structures, a relatively complicated optical setup was used to create multi-beam interference pattern in all these fabrications. Sun *et al.* reported 3D H-PDLC PhCs using UV-curable materials exposed to seven-beam interference generated by a specially designed prism.[34] In this paper, we shall report a one-step fabrication of 3D H-PDLC PhCs with visible-curable materials using a simpler designed prism, which creates a four-beam interference pattern.[35]

2. Experiment

The starting LC/prepolymer mixture syrup used was consisted of 34.8 wt % monomer, trimethylolpropane triacrylate (TMPTA), 8.5 wt % cross-linking monomer, *N*-vinylpyrrollidone (NVP), 0.7 wt % photoinitiator, rose bengal (RB), 1.0 wt % coinitiator, *N*-phenylglycine (NPG), 7.7 wt % surfactant, octanoic acid (OA), all from Sigma-Aldrich, and 47.3 wt % LC, E7, from Merck. The E7 LC used has an ordinary refractive index of $n_o = 1.521$, and a birefringence of $\Delta n = 0.225$. The cell gap was about 30 μm. The exposure time was about 120 s. After exposure, the samples were further cured for 5 minutes using a UV lamp to ensure complete polymerization of the prepolymer. The detailed material preparation and fabrication can be found elsewhere.[25] In our configuration, the polymer refractive index, n_p, is chosen to be as close as possible to the ordinary refractive index, n_o, of LC. Moreover, the birefringence of LC, Δn, is chosen to be as large as possible in order to open large PBGs. The refractive index of the cured polymer is about 1.522.[36] For morphology observation, the tested sample was immersed in liquid nitrogen for easy cleaving and then soaked in ethanol for at least 12 h to remove LC. After drying, the morphology was examined by atomic force microscopy (AFM) and scanning electron microscopy (SEM), respectively. To measure the response time, a He–Ne laser beam operating at 543 nm was normally incident on the sample, and the diffraction was detected by a photodetector. A square waveform voltage from a high voltage amplifier/function generator (Trek 609E-6-FG) was applied on the sample. During the measurement, the photodetector and voltage signals were fed into two different channels of an oscilloscope (Agilent 54641A). From the waveforms captured by the oscilloscope, the rising and falling times were extracted.

The optical setup for the fabrication is schematically illustrated in Fig. 1(a). A laser beam is collimated firstly and

*E-mail address: exwsun@ntu.edu.sg

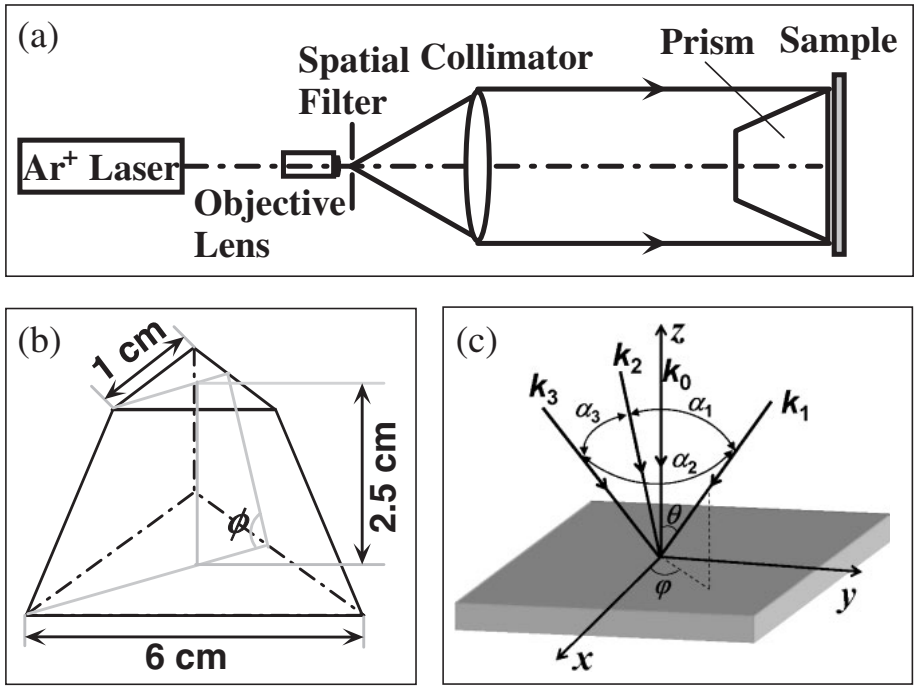

Fig. 1. The schematic of the optical setup (a), specially designed prism (b), and four-beam interference configuration (c).

then impinged normally onto the specially designed prism [Fig. 1(b)], which is made of BK7 glass. The side lengths of top- and bottom-surfaces (isosceles triangle) are 1 and 6 cm, respectively, and the height is 2.5 cm. Emerging from the prism are one directly transmitted beam $\boldsymbol{k}_0$ in the center and three side beams, $\boldsymbol{k}_1$, $\boldsymbol{k}_2$, and $\boldsymbol{k}_3$, by the refraction from three tilted side surfaces of the prism, as shown in Fig. 1(c). These four beams overlap at the bottom surface of the prism and interfere with each other. A cell filled with the LC/prepolymer mixture is attached onto the center of the bottom surface using an index-matched liquid to record the interference pattern. During the recording process, monomers polymerize first in the area with higher exposure intensity. As a result, spatial gradients in chemical potential are established, which produces a diffusion of monomers (and other reactants) into the high intensity regions, and a counter-diffusion of LCs into the low intensity regions. Finally, a 3D structure is formed inside the cell. The use of single prism in the fabrication setup leads to multiple beams generation and interference at the same time, and thus decreases the complexity of the alignment of optics. More importantly, the setup is self-adaptive, i.e., the effect of the external vibration during the fabrication process is minimized.

3. Simulations

The electrical field distribution of a multi-beam interference can be generally described by

$$I(\boldsymbol{r}) = \left[\sum_{j=1}^{n} \boldsymbol{E}_j(\boldsymbol{r}) \exp(i\boldsymbol{k}\cdot\boldsymbol{r} + i\phi_j)\right]\left[\sum_{j=1}^{n} \boldsymbol{E}_j^*(\boldsymbol{r}) \exp(-i\boldsymbol{k}\cdot\boldsymbol{r} - i\phi_j)\right]$$
$$= \sum_{j=1}^{n} |\boldsymbol{E}_j|^2 + \sum_{i\neq j}^{n} \boldsymbol{E}_i \cdot \boldsymbol{E}_j^* \exp[i(\boldsymbol{k}_i - \boldsymbol{k}_j)\cdot\boldsymbol{r} + i\phi_{ij}], \quad (1)$$

where $\boldsymbol{E}$ is the amplitude, $\boldsymbol{k}$ is the wave vector, i and j are integers, ϕ_{ij} is the initial phase difference between two incident waves, and $\boldsymbol{r}$ is the position vector. In our experiment, the beam vectors of the four beams generated by the prism can be written as:

$$\hat{\boldsymbol{k}}_0 = \hat{\boldsymbol{e}}_z, \quad (2)$$
$$\hat{\boldsymbol{k}}_1 = \sin\theta\cos\varphi_1\hat{\boldsymbol{e}}_x + \sin\theta\sin\varphi_1\hat{\boldsymbol{e}}_y + \cos\theta\hat{\boldsymbol{e}}_z, \quad (3)$$
$$\hat{\boldsymbol{k}}_2 = \sin\theta\cos\varphi_2\hat{\boldsymbol{e}}_x + \sin\theta\sin\varphi_2\hat{\boldsymbol{e}}_y + \cos\theta\hat{\boldsymbol{e}}_z, \quad (4)$$
$$\hat{\boldsymbol{k}}_3 = \sin\theta\cos\varphi_3\hat{\boldsymbol{e}}_x + \sin\theta\sin\varphi_3\hat{\boldsymbol{e}}_y + \cos\theta\hat{\boldsymbol{e}}_z, \quad (5)$$

where $\hat{\boldsymbol{k}}$ is unit wave vector, $\hat{\boldsymbol{e}}$ is unit coordinate vector, θ is the angle between the three refracted laser beams and z-axis, which is determined by the cutting angle of the prism, ϕ, and φ is the angle between the projection of laser beam on x–y plane and x-axis (Fig 1). The resulting spatial distribution of the interference pattern is determined by the angles θ, α_1, α_2, and α_3. In this paper, α_1, α_2, and α_3 are fixed at 120° and the cutting angle ϕ for the prism is 60°. Substituting eqs. (2)–(5) into eq. (1) with supposed $\varphi_1 = 180°$, $\varphi_2 = -60°$, and $\varphi_3 = 60°$, we have

$$
\begin{aligned}
I &= (\boldsymbol{E}_0 + \boldsymbol{E}_1 + \boldsymbol{E}_2 + \boldsymbol{E}_3) \cdot (\boldsymbol{E}_0 + \boldsymbol{E}_1 + \boldsymbol{E}_2 + \boldsymbol{E}_3)^* \\
&= |\boldsymbol{E}_0|^2 + |\boldsymbol{E}_1|^2 + |\boldsymbol{E}_2|^2 + |\boldsymbol{E}_3|^2 + 2\boldsymbol{E}_0 \cdot \boldsymbol{E}_1 \cos(kx \sin\theta + kz - kz\cos\theta) \\
&\quad + 2\boldsymbol{E}_0 \cdot \boldsymbol{E}_2 \cos\left(-\frac{1}{2}kx\sin\theta + \frac{\sqrt{3}}{2}ky\sin\theta + kz - kz\cos\theta\right) \\
&\quad + 2\boldsymbol{E}_0 \cdot \boldsymbol{E}_3 \cos\left(-\frac{1}{2}kx\sin\theta - \frac{\sqrt{3}}{2}ky\sin\theta + kz - kz\cos\theta\right) \\
&\quad + 2\boldsymbol{E}_1 \cdot \boldsymbol{E}_2 \cos\left(-\frac{3}{2}kx\sin\theta + \frac{\sqrt{3}}{2}ky\sin\theta\right) \\
&\quad + 2\boldsymbol{E}_1 \cdot \boldsymbol{E}_3 \cos\left(-\frac{3}{2}kx\sin\theta - \frac{\sqrt{3}}{2}ky\sin\theta\right) \\
&\quad + 2\boldsymbol{E}_2 \cdot \boldsymbol{E}_3 \cos(\sqrt{3}ky\sin\theta). \qquad (6)
\end{aligned}
$$

From eq. (6), the periods a, b, and c along the x, y, and z directions can be denoted by the angle θ as

$$a = \frac{\lambda_w}{\sqrt{3}n_{\text{eff}}\sin\theta}, \qquad (7)$$

$$b = \frac{\lambda_w}{n_{\text{eff}}\sin\theta}, \qquad (8)$$

$$c = \frac{\lambda_w}{2n_{\text{eff}}(1-\cos\theta)}, \qquad (9)$$

where λ_w is the writing wavelength, n_{eff} is the effective refractive index of the recording materials. In our experiment, $\lambda_w = 514.5\,\text{nm}$, assuming $n_{\text{eff}} = 1.59$ according to the LC concentration in the homogeneous PDLCs, $\theta = 24.1^\circ$, we can theoretically obtain $a = 458\,\text{nm}$, $b = 792\,\text{nm}$, and $c = 1856\,\text{nm}$.

4. Results and Discussion

With the four-beam intensity ratio of 3 : 1 : 1 : 1 estimated, Fig. 2 shows the theoretically calculated 3D pattern of the spatial intensity distribution of the four-beam interference. Therefore, the PBGs can be easily engineered by changing the cutting angle of the prism. In our experiment, the intensities of the four beams $\boldsymbol{k}_0$, $\boldsymbol{k}_1$, $\boldsymbol{k}_2$, and $\boldsymbol{k}_3$ are 58, 21, 22, and 21 mW/cm^2, respectively, which is very close to the estimated ratio. Figures 3(a) and 3(b) show the AFM images of the surface morphologies with different scanning areas of 10×10 and $4 \times 4\,\mu\text{m}^2$ respectively. Figures 4(a) and 4(b) show respectively the SEM images of the surface and the cross section for the sample, which are in good agreement with the simulation pattern. It can be clearly seen from Figs. 3 and 4 that the surface structure is a

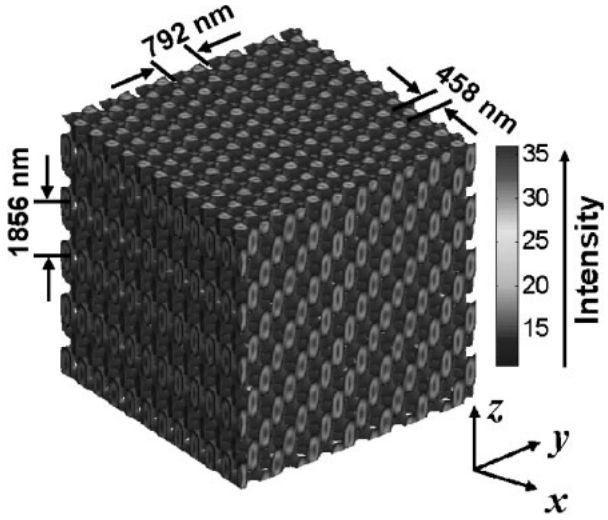

Fig. 2. The simulated 3D four-beam interference pattern. The theoretically calculated periods along the x-, y-, and z-directions are also shown. The color bar shows the intensity distribution.

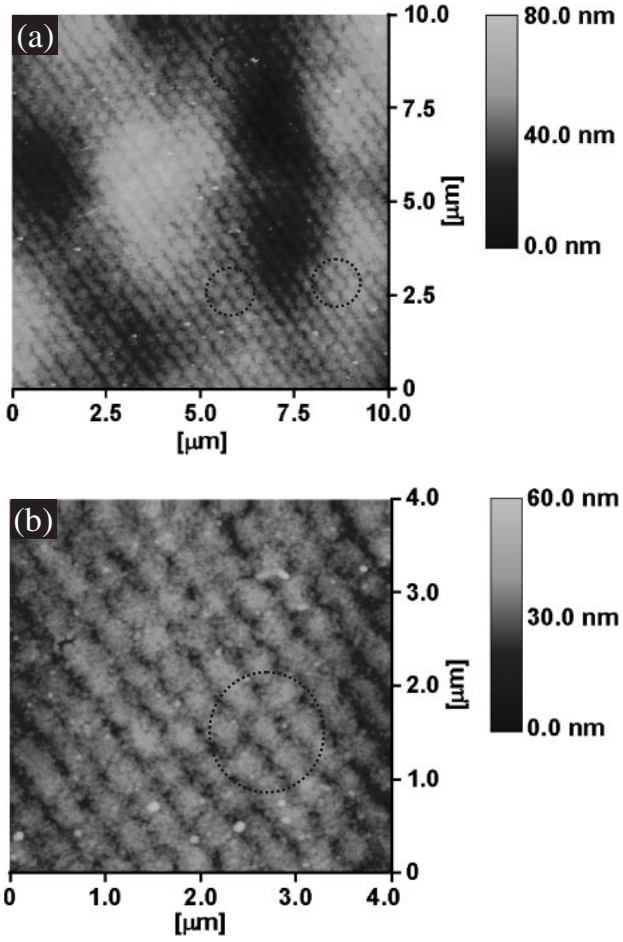

Fig. 3. Surface AFM images of the 3D H-PDLC PhC sample in an area of (a) 10×10 and (b) $4 \times 4\,\mu\text{m}^2$. The hexagonal structures are indicated in the dashed circles.

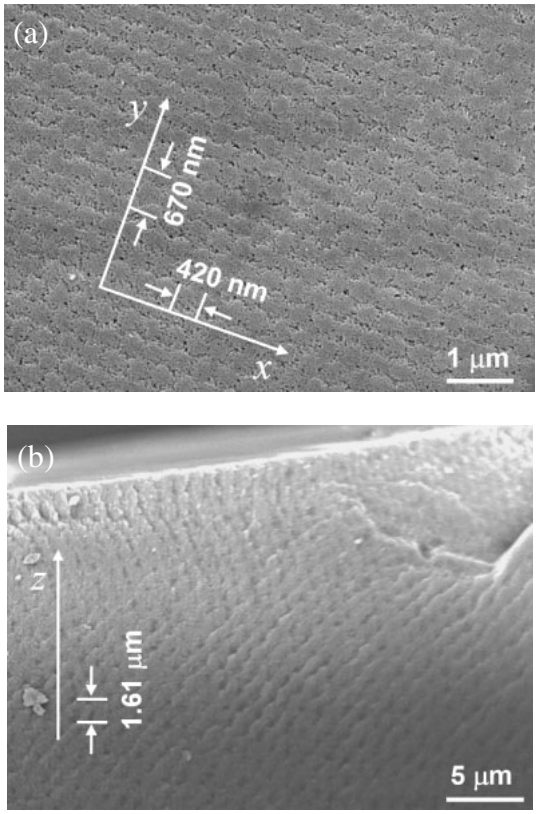

Fig. 4. SEM images of the surface (a) and cross section (b) of the 3D H-PDLC PhC sample. The arrows indicate the *x*-, *y*-, and *z*-directions as defined in Fig. 2.

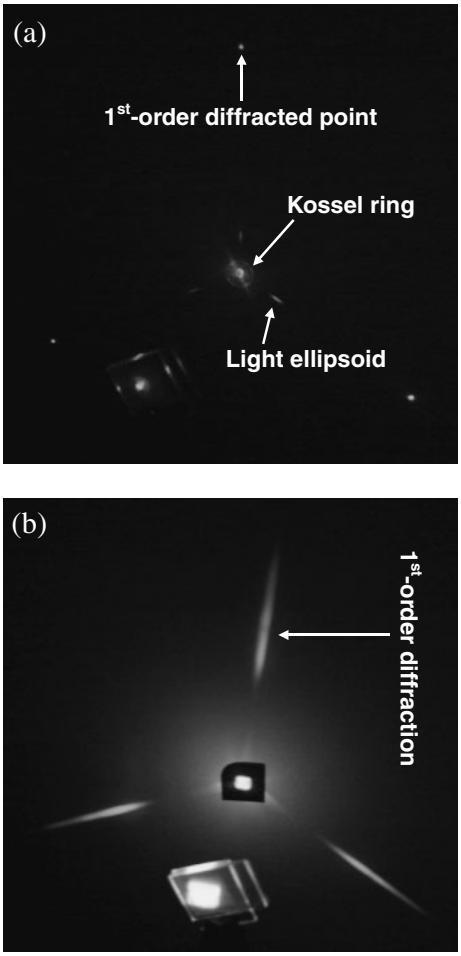

Fig. 5. Diffraction patterns of the H-PDLC PhCs produced by (a) a normally incident He–Ne laser beam, and (b) a broadband white beam.

triangular lattice with a period of about 420 ± 20 nm, which is in good agreement with the theoretical calculation according to the geometrical structure (Fig. 2), considering the general 5–10% volume shrinkage for the acrylate monomer during the photo-induced polymerization.[19,27)]

Figures 5(a) and 5(b) show respectively the visible diffraction pattern produced by a normally incident He–Ne laser beam operating at 543 nm and a broadband white beam for our 3D PhC sample fabricated. From Fig. 5(a), we can see that three first-order diffracted points are reconstructed when a laser beam is normally incident on the sample. It is worth mentioning that three weak light ellipsoids in Fig. 5(a) are induced by the edges of the top surface of the prism. A Kossel ring is also observed in the center of the diffraction pattern, which may be caused by the interference between the impinging four beams and the scattered light. Due to a decreased period, the white light diffraction exhibits a much larger dispersion [Fig. 5(b)] compared to that of the 2D H-PDLC PhCs reported in ref. 37.

For H-PDLC PhCs, a distinct advantage is that they can be tuned by applying a voltage, i.e., the PBGs of H-PDLC PhCs can be changed dynamically. For example, along *z*-axis direction, due to the refractive index difference between the polymer matrix and the LCs, there are PBGs opened in the 3D H-PDLC PhCs. Upon applying a voltage, the LC molecules will re-orientate along the electric field direction, i.e., *z*-axis direction. The normally incident light only sees the ordinary refractive index n_o of the LCs, which is almost equal to the refractive index of the polymer matrix. As a result, the H-PDLC PhC becomes a homogeneous medium,

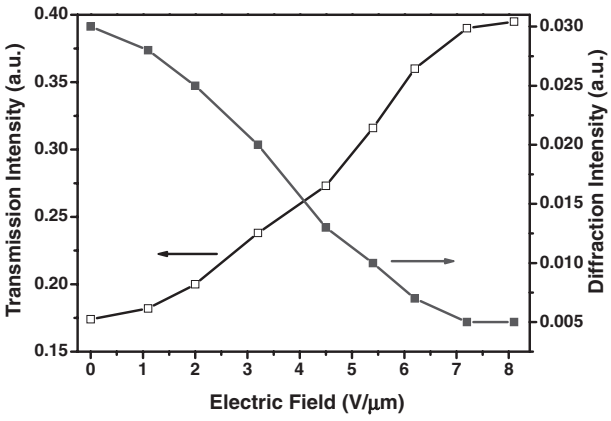

Fig. 6. Diffraction and transmission intensities as functions of applied voltage.

and the PBGs are closed along *z*-axis direction. Therefore, the PBGs could be electrically tuned in H-PDLC photonic structures. Figure 6 shows the changes of the diffraction and the transmission intensity as functions of applied voltage. From Fig. 6, we can see that, with the increase of applied voltage, the diffraction intensity decreases, while the transmission intensity increases, due to the refractive indices matching between the LC and polymer matrix, indicating a PBG tuning in this H-PDLC structure. The switching electric

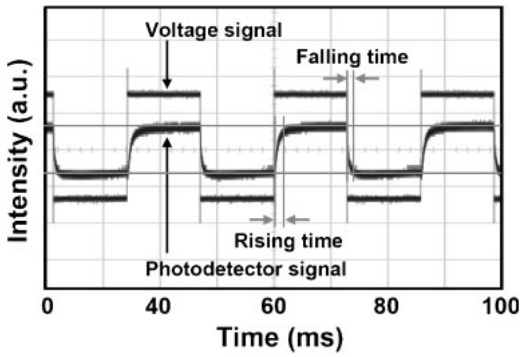

Fig. 7. Measured electro-optical response of the 3D H-PDLC PhC.

field is about 7.2 V/μm, which is much lower than that reported in a similar structure.[34] Due to the large LC concentration used in our experiment, the driving voltage decreases much compared to the low LC concentration case reported previously.[25,37]

Figure 7 shows the measured electro-optical response time when the sample was driven by a square voltage of 185 V_{rms} (6.2 V/μm) with a frequency of 20 Hz. From Fig. 7, the rising time (10–90% intensity changed) and the falling time (90–10% intensity changed), are about 1.75 and 1.09 ms, respectively. The response time is faster compared to thiol-ene (UV-curable) based H-PDLCs.[38]

5. Conclusions

In conclusion, electrically tunable 3D H-PDLC PhCs were fabricated using a specially designed prism. Its diffraction and electrically tunable properties were investigated. It showed fast electro-optical response. Compared to conventional holography, the use of single prism decreases the optics complexity greatly and offers a single-step fabrication, which is self-adaptive against vibration. In addition, the PhC structures can be easily engineered by changing the cutting angle of the prism. Such kind of H-PDLC PhCs can be potentially useful in tunable lasers and superprism effect devices.

1) E. Yablonovitch: Phys. Rev. Lett. **58** (1987) 2059.
2) S. John: Phys. Rev. Lett. **58** (1987) 2486.
3) Y.-J. Lee, S.-H. Kim, J. Huh, G.-H. Kim, Y.-H. Lee, S.-H. Cho, Y.-C. Kim, and Y. R. Do: Appl. Phys. Lett. **82** (2003) 3779.
4) S.-Y. Lin, E. Chow, V. Hietala, P. R. Villeneuve, and J. D. Joannopoulos: Science **282** (1998) 274.
5) B.-K. Min, J.-E. Kim, and H. Y. Park: Appl. Phys. Lett. **86** (2005) 011106.
6) M. D. B. Charlton, S. W. Roberts, and G. J. Parker: Mater. Sci. Eng. B **49** (1997) 155.
7) Y. A. Vlasov, X.-Z. Bo, J. C. Sturm, and D. J. Norris: Nature **414** (2001) 289.
8) E. Özbay, E. Michel, and G. Tuttle: Appl. Phys. Lett. **64** (1994) 2059.
9) M. Campbell, D. N. Sharp, M. T. Harrison, R. G. Denning, and A. J. Turberfield: Nature **404** (2000) 53.
10) V. Y. Miklyaev, C. D. Meisel, and A. Blanco: Appl. Phys. Lett. **82** (2003) 1284.
11) D. N. Sharp, M. Campbell, and R. E. Dedman: Opt. Quantum Electron. **34** (2002) 3.
12) L. Z. Cai, X. L. Yang, and Y. R. Wang: J. Opt. Soc. Am. A **19** (2002) 2238.
13) I. Divliansky, T. S. Mayer, K. S. Holliday, and V. H. Crespi: Appl. Phys. Lett. **82** (2003) 1667.
14) D. C. Meisel, M. Diem, M. Deubel, F. Perez-Willard, S. Linden, D. Gerthsen, K. Busch, and M. Wegener: Adv. Mater. **18** (2006) 2964.
15) Y. K. Lin, D. Rivera, Z. Poole, and K. P. Chen: Appl. Opt. **45** (2006) 7971.
16) S. Yang, M. Megens, J. Aizenberg, P. Wiltzius, P. M. Chaikin, and W. B. Russel: Chem. Mater. **14** (2002) 2831.
17) G. Alagappan, X. W. Sun, P. Shum, and M. B. Yu: Opt. Lett. **31** (2006) 1109.
18) S.-I. Inoue and Y. Aoyagi: Phys. Rev. Lett. **94** (2005) 103904.
19) T. J. Bunning, L. V. Natarajan, V. P. Tondiglia, and R. L. Sutherland: Annu. Rev. Mater. Sci. **30** (2000) 83.
20) K. Tanaka, K. Kato, M. Date, and S. Sakai: SID Int. Symp. Dig. Tech. Pap. **26** (1995) 267.
21) G. P. Crawford, T. G. Fiske, and L. D. Silverstein: SID Int. Symp. Dig. Tech. Pap. **27** (1996) 99.
22) T. J. Bunning, L. V. Natarajan, R. L. Sutherland, and V. P. Tondiglia: SID Int. Symp. Dig. Tech. Pap. **31** (2000) 121.
23) L. H. Domash, T. Chen, B. N. Gomatam, C. M. Gozewski, R. L. Sutherland, L. V. Natarajan, V. P. Tondiglia, T. J. Bunning, and W. W. Adams: Proc. SPIE **2689** (1996) 188.
24) L. H. Domash, Y.-M. Chen, C. M. Gozewski, P. O. Haugsjaa, and M. Oren: Proc. SPIE **3010** (1997) 214.
25) Y. J. Liu, X. W. Sun, J. H. Liu, H. T. Dai, and K. S. Xu: Appl. Phys. Lett. **86** (2005) 041115.
26) D. E. Lucchetta, L. Criante, O. Francescangeli, and F. Simoni: Appl. Phys. Lett. **84** (2004) 837.
27) R. Jakubiak, V. P. Tondiglia, L. V. Natarajan, R. L. Sutherland, P. Lloyd, T. J. Bunning, and R. A. Vaia: Adv. Mater. **17** (2005) 2807.
28) Y. J. Liu, X. W. Sun, P. Shum, H. P. Li, J. Mi, W. Ji, and X. H. Zhang: Appl. Phys. Lett. **88** (2006) 061107.
29) M. J. Escuti, J. Qi, and G. P. Crawford: Appl. Phys. Lett. **83** (2003) 1331.
30) S. P. Gorkhali, S. G. Cloutier, and G. P. Crawford: Opt. Lett. **31** (2006) 3336.
31) R. Sutherland, V. Tondiglia, L. Natarajan, S. Chandra, D. Tomlin, and T. J. Bunning: Opt. Express **10** (2002) 1074.
32) V. P. Tondiglia, L. V. Natarajan, R. L. Sutherland, D. Tomlin, and T. J. Bunning: Adv. Mater. **14** (2002) 187.
33) M. J. Escuti and G. P. Crawford: Mol. Cryst. Liq. Cryst. **421** (2004) 23.
34) X. H. Sun, X. M. Tao, T. J. Ye, P. Xue, and Y.-S. Szeto: Appl. Phys. B **87** (2007) 65.
35) L. J. Wang, Y. C. Zhong, C. T. Chan, K. S. Wong, and G. P. Wang: Appl. Phys. Lett. **86** (2005) 241102.
36) Y. J. Liu, X. W. Sun, H. T. Dai, J. H. Liu, and K. S. Xu: Opt. Mater. **27** (2005) 1451.
37) Y. J. Liu and X. W. Sun: Appl. Phys. Lett. **89** (2006) 171101.
38) A. F. Senyurt, G. Warren, J. B. Whitehead, Jr., and C. E. Hoyle: Polymer **47** (2006) 2741.